Grain-boundary sliding in nanocrystalline fcc metals

H. Van Swygenhoven and P. M. Derlet
Paul Scherrer Institute, 5232 Villigen, Switzerland
(Received 8 March 2001; revised manuscript received 21 June 2001; published 20 November 2001)

Molecular-dynamics computer simulations of a model Ni nanocrystalline sample with a mean grain size of 12 nm under uniaxial tension is reported. The microscopic view of grain-boundary sliding is addressed. Two atomic processes are distinguished in the interfaces during sliding: atomic shuffling and stress-assisted free-volume migration. The activated accommodation processes under high-stress and room-temperature conditions are grain-boundary and triple-junction migration, and dislocation activity.

DOI: 10.1103/PhysRevB.64.224105 PACS number(s): 62.20.Fe, 02.70.Ns

I. INTRODUCTION

Grain-boundary sliding (GBS) is a deformation process that plays an important role in creep and fine-structure superplasticity.[1] It is well known that the grain-boundary (GB) network demands accommodation of GBS, which can be manifested in different ways such as migration of the interface, migration of triple junctions, grain rotation, and dislocation activity in the grain boundary itself or by means of lattice dislocations. The activated accommodation process has an influence on the deformation rate and, therefore, GBS is faster in bicrystals than in polycrystalline specimens. The occurrence of cooperative grain-boundary sliding, i.e., sliding of grain groups as an entity, has also been observed.[2,3] It has been suggested that this is coupled to cooperative grain-boundary migration and grain-boundary rotation.[4,5]

Superplastic behavior is usually observed at high temperature, when vacancy diffusion provides a mechanism for mass transport able to relieve the stress accumulation in the grain-boundary regions or triple junctions. A wavy slide channel leads to the formation of cavity and overlap zones, similar to the nonconservative motion of dislocations,[6] a process that requires vacancy diffusion to be removed. Since superplasticity is a grain size-dependent phenomenon, the possibilities of high strain-rate superplasticity and/or low-temperature superplasticity in nanocrystalline materials has been discussed. Recently, both low-temperature and high strain-rate superplasticity have been observed in nanocrystalline Ni_3Al at 470 °C with mean grain sizes of 50 nm, and in pure nanocrystalline Ni at 0.36 of the melting point with mean grain sizes of 20 nm.[7,8]

Molecular-dynamics (MD) investigations of nanocrystalline material have proven to be a valuable and complementary tool for the investigation of grain-boundary structure and the atomic-level detail of intergrain and intragrain plastic-deformation mechanisms.[9–16] In MD computer simulations of plasticity, the time scale is too short and the temperature too low to observe effects due to general long-range diffusion. However, these restrictions do not exclude some form of stress-assisted atomic activity in the grain-boundary region, especially since high values of stress are applied in simulation experiments due to the computational-time limitations. This means that changes in grain-boundary shape and structure can still be expected, however, due to the short time scales accessible by simulation, superplasticity cannot be directly observed. Only the very early stages of deformation can be studied by the present method.

In previous works[9–13] we simulated the mechanical behavior of two model nanocrystalline fcc metals, Ni and Cu, under constant uniaxial stress. We observed that at the smallest grain sizes all deformation is accommodated in the grain boundaries, at larger grain sizes, however, intragrain dislocation activity is detected. Stacking faults are produced by the passage of partial dislocations generated and absorbed in opposite grain boundaries. We showed also that the critical grain size below which all deformation is accommodated in the grain boundary decreases with decreasing stacking fault energy. We proposed that an atomistic jump process controls plasticity below that critical grain size. With a set of simple assumptions based on the observations: (i) there is no damage accumulation during deformation, (ii) macroscopic displacement is the result of grains sliding against each other with a general nonlinear viscous behavior, and (iii) there is no contribution to plasticity from the grain interior, we arrived at a picture of a standard stress-assisted activation process. To incorporate all the relevant variables into the problem, we considered the following arguments:

1. In a sample with grain size d, the total surface per unit volume is proportional to $1/d$.

2. The fraction of interfaces of a given three-dimensional array under a particular stress condition that contributes to plastic deformation is constant regardless of grain size. Equivalently, the scale does not affect the geometric factors that project the applied stress into the active interfaces.

3. Increasing the total interface surface increases the slip channels that contribute to total strain in the same way as parallel dashpots do in a mechanical model of viscoelastoplastic solid.

Under these assumptions, we proposed the following relationship for the strain rate as a function of grain size, temperature, and stress,

$$\dot{\varepsilon} = \frac{\dot{d}_0}{d} \exp\left(-\frac{U}{k_b T}\right) \sinh\left(\frac{\sigma V}{k_b T}\right). \tag{1}$$

Here $\dot{d}_0$ is a constant that can be interpreted as the characteristic elongation rate of a grain of size d, U and V are the activation energy and volume, and σ is the applied stress.

 ©2001 The American Physical Society

Despite its simplicity, the activation energy and volume give some indication about the underlying microscopic mechanism. For a computer modeled Ni,[10] we obtained $V=16$ Å^3, in the range of one atomic volume, and $U=0.2$ eV. These values have to be considered as mean values of a distribution of activation energies and volumes. When comparing to the self-interstitial migration energy in crystalline Ni (0.15 eV,[17]) and the migration energy for vacancies in crystalline Ni (1.3 eV,[18]), a value that is expected to be much lower in grain boundaries, the obtained activation energy suggests that the intragrain deformation process is governed by individual jump events, each contributing to minute amounts of strain.

In a more recent work, Conrad and Narayan[19] use precisely these hypotheses to give further interpretation to the term $\dot{d}_0$ in Eq. (1). From the same underlying assumption of a microscopic process, they find that the rate-limiting factor is $N_\nu Ab\nu$, with N_ν, the number of atoms per unit volume where thermal activation can occur; A, the area swept per jump; b, the atomic size; and ν, the jump frequency. With $N_\nu=\delta/(db^3)$ (assumptions 1 and 2) and the further assumption that δ (the GB width) is equal to $3b$, they obtain $\dot{d}_0=6b\nu$.

The ability of Eq. (1) to fit a large set of experimental data (see Ref. 19) strongly supports the view that the plastic deformation mechanism in nanocrystalline metals is GBS resulting from the combined action of individual atomic jump processes. At finite temperature this mechanism is controlled by an activation enthalpy related to diffusion in the GB with an activation volume comparable to atomic sizes. In qualitative terms, it means that when a homogeneous shear stress is applied across the interface between two grains, the local heterogeneous stress field makes each atom feel a different value of the net force (external plus internal) acting on them. At every instant of time, depending on both the specific environment of each atom and on thermal fluctuations, a certain number of atoms will reach the conditions necessary to pass their saddle-point configuration and migrate to a new location, relaxing the corresponding local stress. In this way a local contribution is made to the total plastic strain. The combination of all these localized, randomly distributed processes, leads to a homogeneous slide of grains with respect to each other.

The nature of such atomic processes still requires a precise atomistic description. For example Sutton and Balluffi[20] have defined the process in which an atom transfers directly from one grain to another, without the creation of point defects, as uncorrelated shuffling. Atoms can, however, also be transported across the interface via diffusion of point defects that are created and destroyed at different places in the interface. Such atomic activity can also involve several atoms and be responsible, for example, for the migration of grain-boundary line defects such as pure steps. This largely uncorrelated atomic activity has been referred to as ''civilian'' style shuffling. True correlated grain-boundary atomic activity involving many atoms can occur via the motion of interfacial dislocations either by glissile activity, climb or glide. This highly collective atomic activity has been referred to as ''military'' style shuffling.

In this paper we first address the atomic view of GBS under a constant tensile stress, in a model nanocrystalline Ni sample with an average grain size of 12 nm, aiming at identifying some possible atomic processes occurring during deformation. We then show how the grain-boundary network accommodates for the observed sliding that in the case of the 12 nm sample also includes dislocation activity. In the present work we are not concerned whether the origin of GBS is directly from the applied stress or induced by deformation of the other surrounding grains. Thus the precise classification of GBS via ''proper'' and ''induced'' sliding (see for example, Ref. 21) will not be addressed. Further, the mechanical properties of grain boundaries are a complex phenomenon that not only depends on parameters such as stress, strain, and temperature, but also on the characteristics of the interfaces that are involved and the nature of the grain-boundary network. We note that in a former paper[13] we have studied the structure of grain boundaries used in the present samples, focusing particularly on the possibility of finding regions in the boundary exhibiting order and structural units normally expected for high-angle boundaries. Those results suggested that grain-boundary structures in nanocrystalline materials are not that different from those found in larger grain polycrystals, which is in agreement with a variety of experimental evidence.[22,23]

II. COMPUTATIONAL TECHNIQUE

Nanocrystalline samples were created by constructing nanograins at random locations and crystallographic orientations according to the Voronoi construction.[24] Samples were then relaxed to a minimum enthalpy at 300 K for 50–100 ps using isokinetic molecular dynamics. The relaxed structure has a final density between 96% and 97% of the perfect crystalline value depending on the mean grain size. Each sample contains 15 randomly oriented grains in such a way that different types of interfaces appear, with all types of misfit from low angle to high angles. A more detailed description of this procedure can be found in Refs. 9–13.

Molecular dynamics was performed within the Parrinello-Rahman approach,[25] with periodic boundary conditions and fixed orthorhombic angles. The simulations are performed at 300 K under an applied uniaxial stress of 2.6 GPa for the 12 nm sample. After an initial transient period, the strain rate can be approximated by a linear function of time, reaching a value of $\sim 10^7$.

We used the second-moment (tight-binding) potential of Cleri and Rosato for describing the atomic interactions for a model fcc Ni.[26] In order to assess the dependence of our results on the interatomic potentials we have tested two other embedded atom potentials.[27,28] These more recent models have been fitted to extensive data bases of Ni properties obtained from both experiment and *ab initio* calculations, and are expected to be more reliable in situations far from equilibrium. The same qualitative results have been obtained with all potentials tested.

To analyze the grain boundaries we calculate the local crystalline order according to the Honneycutt and Andersen analysis,[29] a technique based on determining the configuration of the common neighbors of a selected atom pair. For more details about this procedure applied in our simulations we refer to Ref. 13. Using this analyzing technique we defined four different classes of atoms to which a different color is attributed: gray represents fcc atoms, red represents first nearest-neighbor hcp coordinated atoms, green represents other 12 coordinated, and blue represents non-12 coordinated atoms. This tool proved to be very helpful in the visualization of the grain-boundary structures and is helpful in identifying twin planes and stacking faults.[11,13]

III. RESULTS

Our sample contains a wide distribution of GB's, including low-energy dislocation structured boundaries as well as high energy less structured ones.[13] Careful analysis of all grain boundaries during deformation revealed that grain-boundary sliding can be observed in nearly all boundaries, in some, however, to a lesser extent, depending on the characteristics of the boundary itself and on the local stress. During the sliding atomic shuffling is observed. In most cases the free volume already present in GB is the driving force for the observed shuffling. In some cases the atomic shuffling is accompanied by a stress-assisted free-volume migration. As accommodation mechanisms to grain-boundary sliding, GB migration, rearrangements of triple junction, and dislocation emission and glide was observed. Grain rotation was not observed in our simulations. This is probably due to the fact that only the early stages of deformation can be investigated for the applied stresses used in the present work. It is not excluded that rotation will be observed at higher deformation levels. In the following paragraphs we first discuss with the help of two examples the atomic activity in the GB, then we address the accommodation processes.

A. Atomic activity in the grain boundaries

1. Sliding parallel to the GB plane

In Fig. 1 we display a section of the grain boundary between grain number 1 and grain number 14 of the 12 nm sample. The plane of the paper represents a (011) plane for grain 1 and a (-112) plane for grain 14. The atoms are shown at their positions prior to loading and the thickness of the section (perpendicular to the sheet of paper) is four atomic layers. In grain 1 the unit cell is highlighted in yellow, in grain 14 the (111) planes are indicated and also the crystallographic directions [110] and [1-11]. To visualize the relative displacement of atoms in the two grains resulting from approximately 2% plastic deformation, the displacement vectors have been calculated with respect to the (local) center-of-mass coordinate system of the atoms in grain 1. As can be observed GB sliding is approximately parallel to the GB plane and with a significant sliding component in the (111) plane. During sliding we observe within the GB some single events across the grain boundary that can be identified as shuffling of atoms across the interface.

In order to resolve the atomic activity in time, numbers are attributed to those columnar regions (with respect to the viewing direction) taking part in the atomic shuffling. When a load is applied, the atoms occupying regions 1 and 2 (constituting lattice positions in grain 14) slide away increasing the excess free volume at the connecting region between grains 14 and 1. When the atoms in grain 14 have slid by an amount equal to about 50% of the indicated sliding vector, two atoms sitting in region 3 of an (011) plane of grain 1, move in the direction of region 2, transferring free volume into grain 1. The new positions taken by these atoms are again lattice positions of an (011) plane in grain 1. Then a shuffle takes place to refill one of the vacant sites in region 3 by an atom sitting in region 4. Region 4 constitutes lattice positions common to both grain 1 and grain 14. Only a very short time later, a similar process takes place, an atom sitting in region 5 shuffles to region 1. This position is filled up with another atom in region 4, which then in turn is filled up by a shuffle of an atom in region 6. The atom that shuffles towards the GB, is not the fcc (gray atom) represented in region 6, but the blue atom sitting below. This atom is less than an atomic distance away from the GB plane since the GB plane is slightly inclined relative to the viewing direction.

The events described above are a clear example of uncorrelated shuffling during GB sliding. The excess atomic volume, already present in the unloaded GB (especially in these areas where misfit between the crystallographic orientations is adapted) seems to play a dominant role. This example cleary shows that plastic deformation is a result of an interplay between sliding of atomic planes and atomic shuffling across the interface.

2. Sliding nonparallel to the GB

Figure 2 details a relatively sharp grain boundary in which the viewing orientation is such that the misfit network can be visualized in terms of (111) planes in grain 1 and (100) planes in grain 7. The displayed atoms are at their unloaded positions. The plane of atoms labeled ''blue'' contains regions of atomic positions akin to either (111) or (100) planes, whilst the plane of atoms labeled ''red'' contains positions that are predominantly that of the (111) plane of grain 1. In the misfit regions there is increased disorder. Together these planes form an approximate dichromatic pattern when viewed head on. Atomic displacement vectors between the unloaded and loaded sample (at 3% total strain) are also shown. We see that grain 7 undergoes sliding relative to grain 1 with the sliding vector nonparallel to the grain boundary.

Figures 3(a) and 3(b) are views of the grain-boundary constructed from the ''blue'' and ''red'' atomic planes indicated in Fig. 2, their color being appropriately set to which plane they belong to. The positions of the atoms in Fig. 3(a) are those of the loaded sample at the approximate onset of plastic deformation (1.7% total strain), and in Fig. 3(b) they are the atomic positions at 3% total strain. The viewing orientation is now perpendicular to the grain boundary, with the

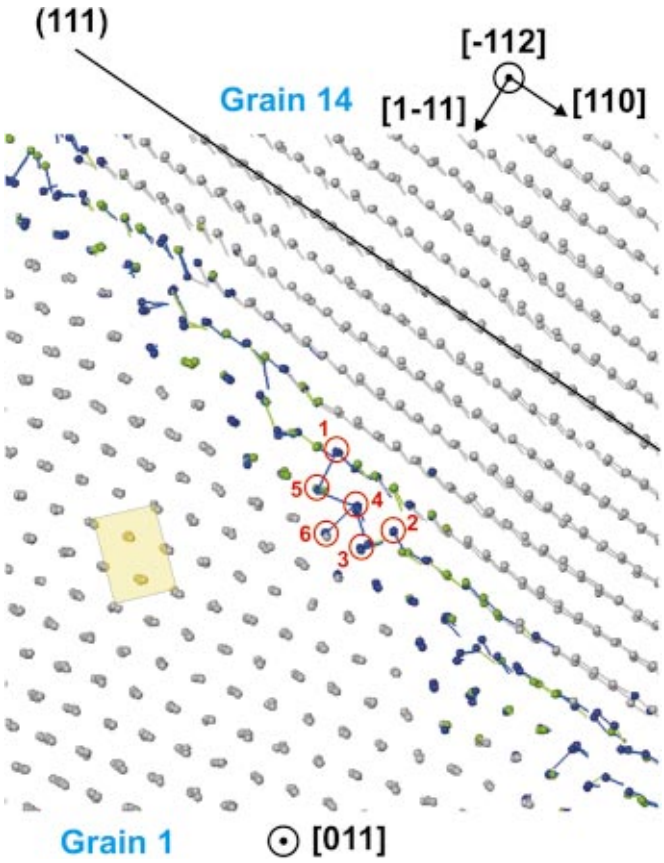

FIG. 1. (Color) A section of the GB between grains 1 and 14. Displacement vectors are shown indicating the change in position between two levels of strain during plastic deformation. Atomic shuffling between the grains can be observed.

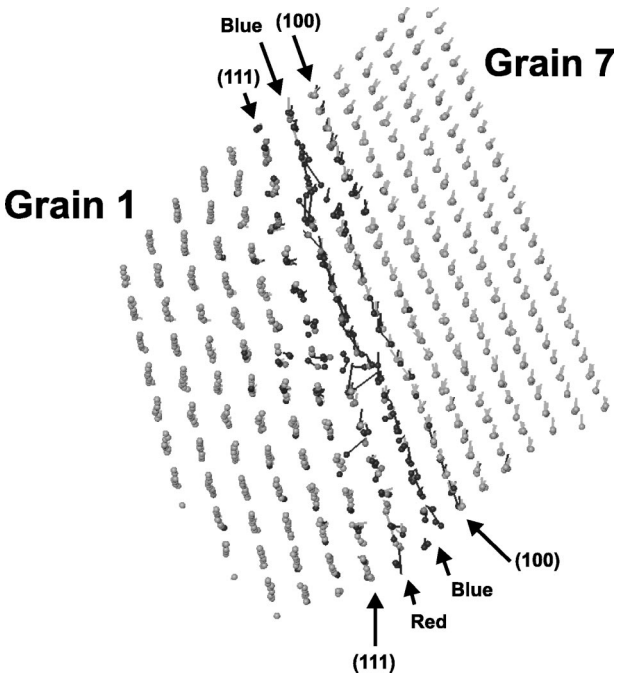

FIG. 2. A section of the GB between grains 1 and 7. For grain 1, (111) atomic planes are shown and for grain 7, (100) planes are shown. Displacement vectors are shown. The atomic planes indicated by "blue" and "red" constitute the misfit of the GB.

plane of red atoms below the plane of blue atoms. We see that the blue plane does indeed contain regions of atomic positions akin to either a (111) plane or a (100) plane. To emphasize this we have added a (111) and (100) mesh to both blue and red planes. Where there is a transition from one local geometry to another, we have distorted the mesh accordingly. This is evidenced by the increased disorder in the atomic positions. The atomic-displacement vectors of these two planes are also shown, their color is set to green and their length equal to the displacement (projected onto the viewing plane) between the sample at the onset of plastic deformation and 3.0% total strain. Thus in Fig. 3(a), the relevant atoms are at the beginning of the displacement vector and in Fig. 3(b), they are at the end. The sliding vector of grain 7 projected onto this viewing plane is indicated by an arrow on the right of the figure. During the sliding some atomic shuffling takes place in the two planes.

We now describe this activity, especially those of the numbered atoms. This information was gained by analyzing a number of samples separated in time over a period of 10 ps. Atom number 1 that initially is in the lower red (111) atomic plane shuffles to the blue (100) plane into a region that, seen from the positions of the surrounding blue atoms, contains increased free volume. In this region there is greater distortion because the blue and the red planes are in closer proximity to each other to form the misfit. Atoms $2a$, $2b$, $2c$, and $2d$ shuffle accordingly, remaining in their original planes. As can be seen in Fig. 3(b), their final positions will coincide with the migration of the grain boundary. Returning to Fig. 3(a), atom 3 moves to the region of free volume created by the movement of atoms $2b$ and $2d$. This in turn creates free volume into which atom $4a$ hops, which then causes a cascade of atomic movement (atoms $4b$, $4c$, etc.) corresponding to the migration of free volume into a nearby triple junction [the upper right corner of Fig. 3(a)].

Figure 3(b) now places the atoms at their final positions, thus at the end of the green displacement vectors. Again, we have drawn a mesh to indicate the local (111) and (100) geometries. Comparison to Fig. 3(a) clearly shows that with the atomic activity just described, there is an increase of the blue (111) plane via atomic reconstruction down and to the right of the figure. In addition, the region of disorder slightly above atom 1 in Fig. 3(a), has shifted down further into the red plane of atoms corresponding to the movement of the misfit region. With the growth of one crystallographic orientation over another, this activity clearly demonstrates GB migration.

In summary, at the atomic level, shuffling and stress-assisted free-volume migration plays an important role in the plastic deformation processes occurring at the GB region.

B. GB network accommodation processes

1. Migration in a "close to" $\Sigma=3$ GB

It is well known that low-energy GB, such as twins, do not readily slide under appropriate shearing stress.[6] Figure

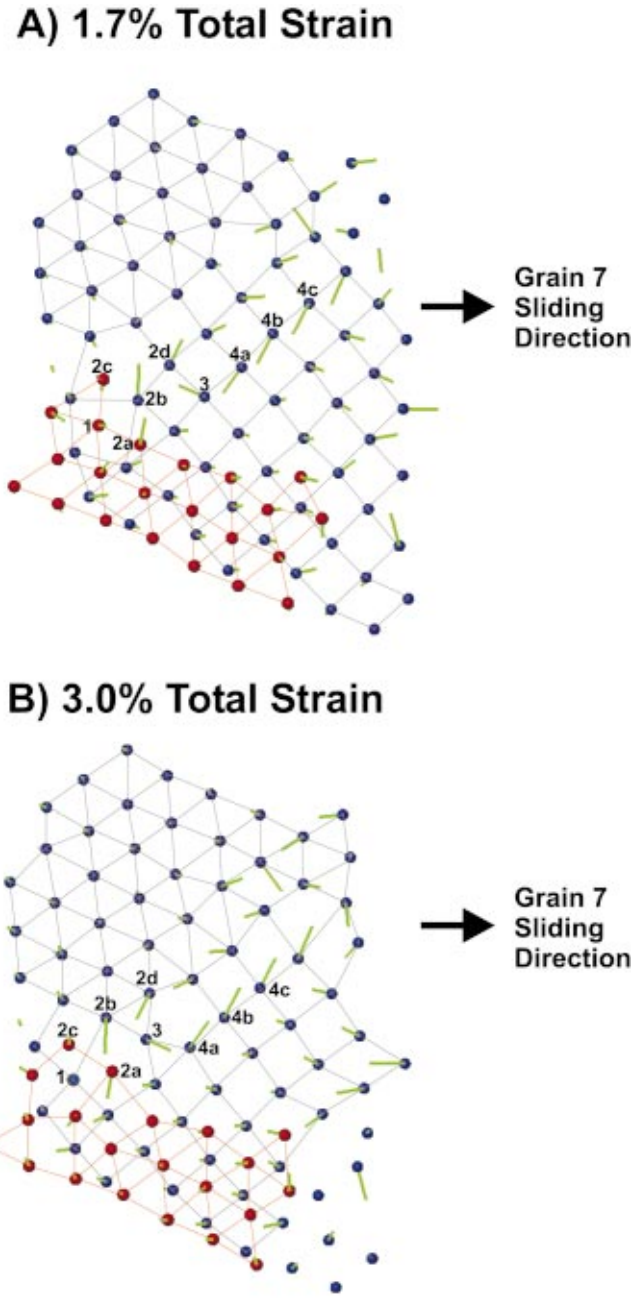

FIG. 3. (Color) View perpendicular to GB detailed in Fig. 2 (''blue'' and ''red'' plane), (A) at a total strain of 1.7% and (B) at a total strain of 3%.

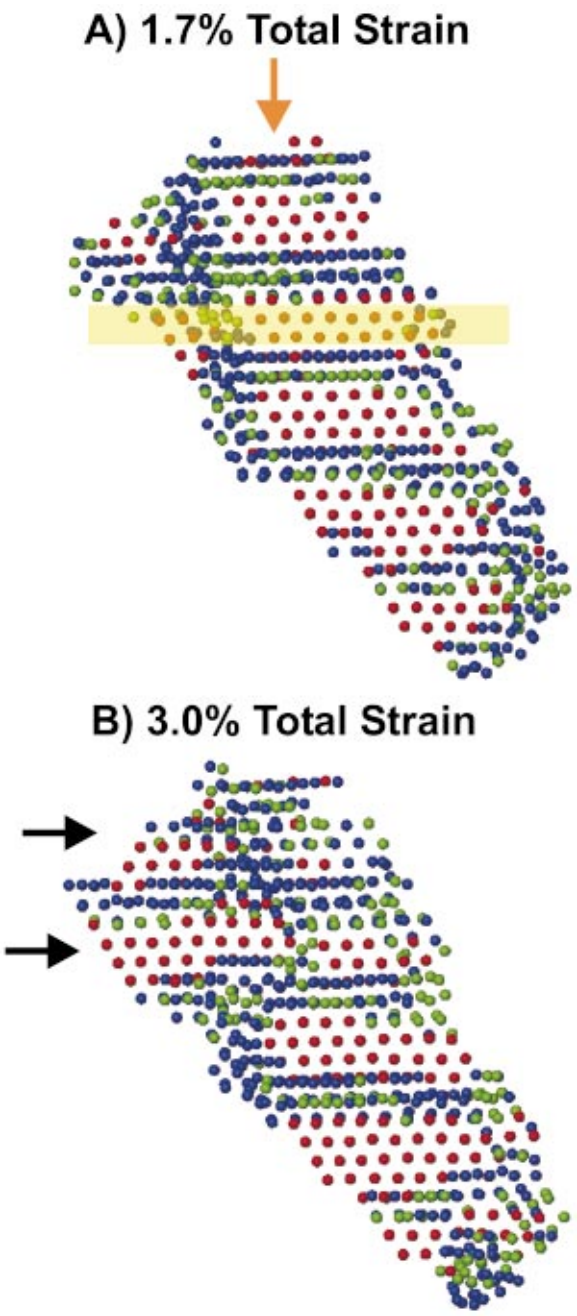

FIG. 4. (Color) Grain boundary with a misorientation close to a $\Sigma=3$ twin, whose structural units can be seen via the red hcp twin planes separated by regions of increased disorder, (A) at a total strain of 1.7% and (B) at 3%. With deformation, migration of the twin regions from the left to the right is observed.

4(a) shows a view perpendicular to a GB plane that is close to an ideal $\Sigma=3$ GB. The figure shows a snapshot of the grain boundary after the sample has been deformed up to 1.7% total strain. This involves most of the elastic part. In this figure fcc atoms are omitted for clarification. The misorientation between these grains (grains 13 and 14) in the unloaded sample is 75°, which is 4.5° more then a $\Sigma=3$ coincidence lattice. The GB is described in detail in Ref. 13. The GB appears as a sequence of structural building blocks, each one formed by a portion of a (111) twin-boundary plane (red atoms) and a step between them, which is a disordered region (blue/green atoms). These steps are themselves located on a (111) plane, 60° from the (111) twin planes, and are pure steps of height equal to three (111) planes. Figure 4(b) represents the same GB but at a total sample deformation of 3% total strain. Inspection of both figures reveals movement of the step from left to right, whose ridge extends down the page, with the corresponding growth of two twin planes from the left to the right [indicated by the two black

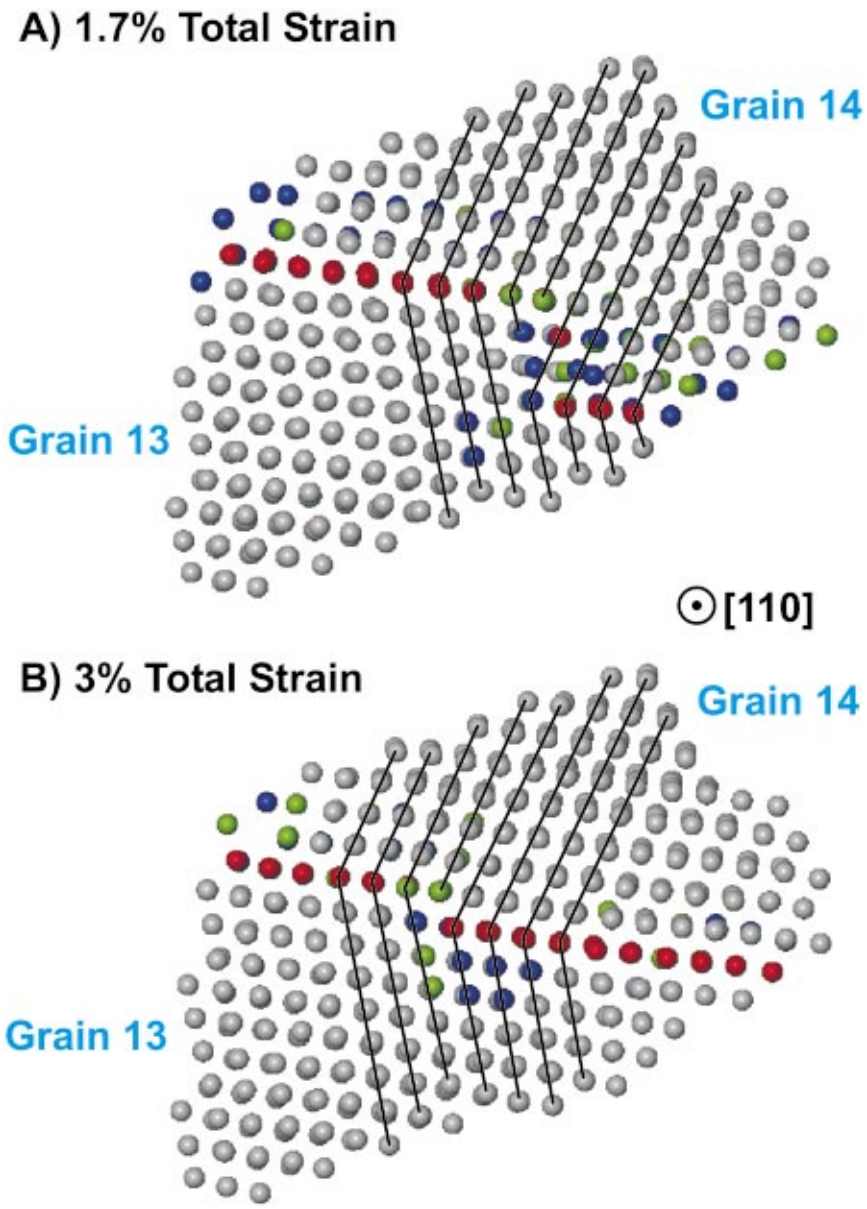

FIG. 5. (Color) A view detailing the nature of the twin-plane migration within the grain boundary shown in Fig. 4, (A) at a total strain of 1.7% and (B) at 3%.

arrows in Fig. 4(b)]. Figures 5(a) and 5(b) are a view of the highlighted atoms [in yellow in Fig. 4(a)] from a side on view in a [110] direction [indicated by the orange arrow in Fig. 4(a)] at the same levels of deformation as in Fig. 4. Here we see that during deformation, along with the step motion there is a migration of the twin, transforming from a pure step (three planes) to a single step of one plane. In Fig. 5(a) we have attempted to indicate the pure step from the perspective of two additional (111) planes as suggested in Ref. 19, the parallel black lines. We note, however, that there is much disorder and local strain, making it difficult to fit directly to a simple (111) geometry. By attempting the same construction in Fig. 5(b), we see that the single step resulting from the migration of the twin plane can be viewed from the perspective of now only one additional (111) plane.

Figure 5 suggests that the migration of the twin plane involves dislocation activity. This is in fact difficult to realize for the case of a twin plane moving only two (111) planes (rather than three) and indeed it was found not to be the case. By analysis of atomic activity within the pure step regions as a function of time during 20 ps of deformation, it was found that a large number of atomic shuffles are responsible for the migration of the more disordered pure step regions displayed in Figs. 4 and 5. Furthermore a mixture of local distortions and minute relative sliding between grains 13 and 14 result in the migration of the twin plane by two atomic (111) planes, involving the collective motion of the atoms in the (111) plane above the initial twin. Figure 6 is an idealized diagram that attempts to indicate the procedure by which this process occurs. It has the same orientation as Fig. 5. In this figure, (111) planes are indicated, with the initial twin, initial pure step, and second twin plane shown. Black circles indicate the idealized *ABC* stacking and thus the initial twin plane. There is minute sliding (of the grains) indicated by the black arrows, which corresponds to the movement

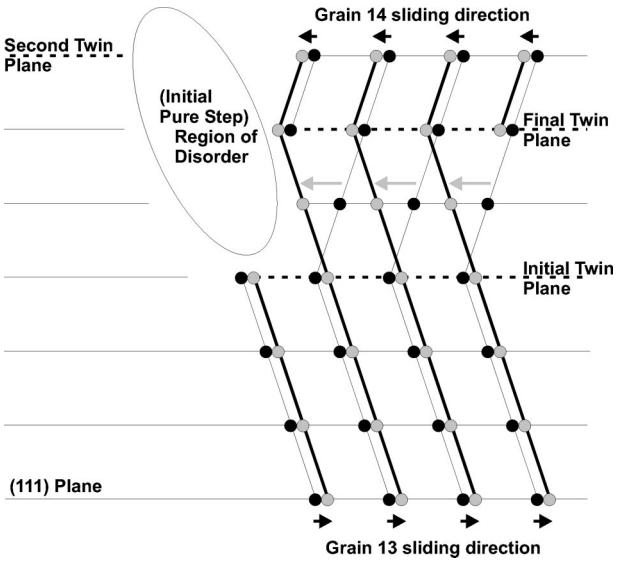

FIG. 6. Schematic of the twin-plane migration shown in Fig. 5. See text for details.

of the atoms (idealized by circles), their final positions being represented by the light gray circles. The movement of the twin plane from the initial to final (111) plane can take place only when the atoms in the middle (111) plane collectively move to the left by a greater distance. This motion is indicated by the three central light gray arrows. In reality it is not just sliding that drives the migration, but also the distortion due to the nearby regions of disorder. The motion of the atoms in the middle (111) plane was observed to be collective within the 3 ps resolution of the temporal analysis. Thus the migration of the boundary is driven by uncorrelated shuffling of atoms in the disordered step, followed by a collective shuffling of atoms in the first (111) plane above the twin.

2. Migration of a triple junction

In Figs. 7(a) and 7(b) we show a triple junction between grains 3, 7, and 15, which slide significantly relative to each other during the deformation. Figure 7(a) is at 1.7% strain and Fig. 7(b) is at 3% strain. Here we see that there is a clear migration of the GB structure particularly between grains 3 and 7, corresponding to a displacement of the triple-junction region by several atomic distances. In Fig. 7(b) at 3% strain, twin hcp planes can be seen due to the emission of a partial dislocation within grain 15. The dislocation is emitted from a region not directly related to the triple junction of present interest. Figure 8 displays the atomic positions at 1.7% strain for the central triple-junction region in a slightly different orientation to emphasize the relative sliding. Also shown are the atomic-displacement vectors between the levels of deformation indicated in Fig. 7, their color being set by the final crystalline order. It can be seen that grains 3 and 7 slide in different directions relative to grain 15. The migration of the grain boundary between grains 3 and 7 is of the order of 3 to 4 atomic planes. Analysis of individual atomic activity using a number of intermediate strains (times) reveal that migration is a result of an interplay between sliding and shuffling events.

3. GBS plus dislocation glide

Figure 9 shows a GB between grain 12 and grain 13 from the 12-nm nanocrystalline sample during deformation. Here the view is perpendicular to the grain-boundary plane in which the plane of the paper represents a (013) plane for grain 12 and a (-123) plane for grain 13. The orientation of a (33-1) plane and of a (1-11) plane of grain 13 are also indicated. To visualize the relative displacement of atoms in the two grains, the displacement vectors have been calculated with respect to the center-of-mass coordinate system of the atoms in grain 12. In this figure, the color of the displacement vectors is taken as the atom's initial crystalline order, and also, the displayed atoms are at their final positions. As can be observed, grain 13 slides relative to grain 12 in a direction more-or-less parallel to the grain-boundary plane that is close to a (33-1) plane. The sliding vector has a large component perpendicular to a (11-1) plane, whereas in Sec. III A 1 the sliding vector was approximately parallel to a (111) plane.

During deformation, at a total strain of about 2.5% (representing a plastic deformation of approximately 0.8%) a partial dislocation is emitted close to the displayed triple junction. This is identified by the twin (red) hcp planes of the associated stacking fault, and can also be evidenced by the change in displacement vector to the right of the stacking fault. The glide plane of the Shockley partial is (11-1); the dislocation line at this time is mainly composed of two segments, aligned approximately along [1-10] and [011] directions, the Burgers vector being $a/6$ [-121]. This dislocation has been analyzed in detail in Refs. 9,11. For the same grain boundary in a 5.2 nm average grain size nanocrystalline Ni sample, only pure sliding with an associated strain field is observed after 3% deformation, and no dislocation emission.

IV. DISCUSSION AND CONCLUDING REMARKS

Careful analysis of the GB structure during sliding under constant tensile load, shows that sliding includes a significant amount of discrete atomic activity, either through uncorrelated shuffling of individual atoms and in some cases shuffling involving several atoms acting with a degree of correlation. In all cases, the excess free volume present in the disordered regions plays an important role. In addition to the shuffling, we have observed hopping sequences involving several GB atoms. This type of atomic activity may be regarded as stress-assisted free-volume migration. Together with the uncorrelated atomic shuffling they constitute the rate controlling process responsible for the GBS. This clearly demonstrates that the activation enthalpy in Eq. (1) will represent an arithmetic mean of the various atomic-level deformation processes occurring in the grain-boundary region.

Sliding is accompanied by stress buildup across neighboring grains. A local stress increase across a grain will lead indirectly to accommodation by GB and triple-junction migration, and dislocation emission and propagation. We note

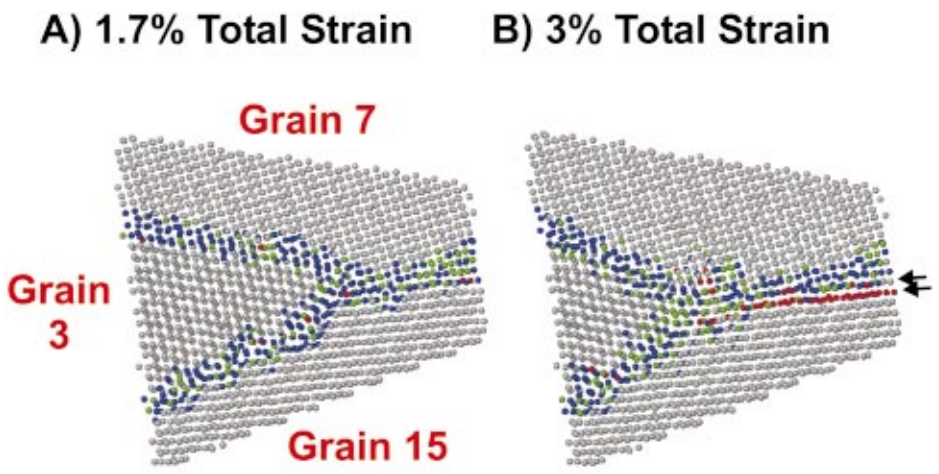

FIG. 7. (Color) An example of triple-junction migration between grains 3, 7, and 15, between two stages of plastic deformation, (A) at a total strain of 1.7% and (B) at 3%.

that previous work has shown that dislocation activity does not take place in samples with smaller mean grain sizes.[11] In the same grain boundary, between grains 12 and 13, no dislocation activity was observed in a 5.2 nm sample. On the other hand, grain size cannot be the only criteria since the GB between grains 12 and 13, and grains 1 and 14 have approximately the same size; the first, however, show dislocation activity and the second only sliding. A quantitative relationship between GB sliding and dislocation activity is not possible from the few cases studied. Moreover it can be expected that the local environment (GB geometry) plays an important role in whether dislocations are emitted or not. Such a problem is fully time dependent requiring detailed temporal analysis of microscopic stresses, GBS and related dislocation activity.

In summary we show in this work the mechanism of GBS at the atomic level in a model nanocrystalline computer-generated Ni sample. Furthermore, the accommodation mechanisms in this regime of high-load and room-temperature conditions, are grain-boundary and triple-junction migration, and dislocation glide, in agreement with the present knowledge for coarser-grain polycrystals. By inspection of a variety of different grain boundaries at the atomic level, uncorrelated atomic shuffling has been identified together with stress-assisted free-volume migration. To-

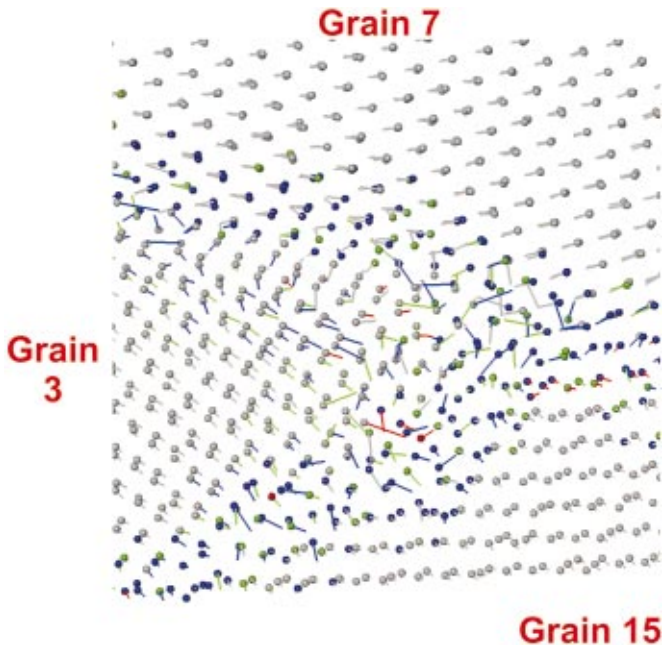

FIG. 8. (Color) A more detailed view of the triple junction shown in Fig. 7 in a slightly different orientation to emphasize the relative sliding between the grains. Atomic displacement vectors are shown with their set to the final atomic crystallinity.

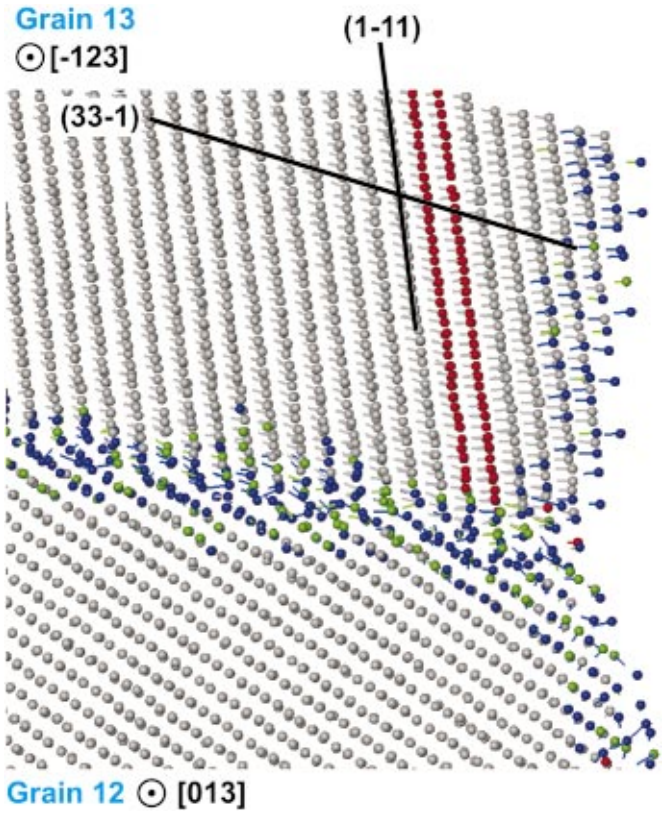

FIG. 9. (Color) A section of the grain boundary belonging to grains 12 and 13. The atomic displacements due to 1.3% plastic strain are indicated, their color being determined by the final atomic crystallinity. At an intermediate strain a partial is emitted in a region close to the triple junction on the right, as indicated by the twin hcp planes.

gether these are believed to constitute the atomic-scale jump processes alluded to in earlier work involving a nonlinear viscosity model for plastic deformation in nanocrystalline material.[10]

ACKNOWLEDGMENT

The authors acknowledge support from the Swiss NSF (2000-056835.99).

[1] R. C. Gifkins, Metall. Trans. A **7A**, 1225 (1976).
[2] V. V. Astanin, O. A. Kaibyshev, and S. N. Faizova, Scr. Metall. Mater. **25**, 2663 (1991).
[3] H. S. Yang, M. G. Zelin, R. Z. Valievand, and A. K. Mukherjee, Scr. Metall. Mater. **25**, 1707 (1992).
[4] M. G. Zelin and A. K. Mukherjee, Acta Metall. Mater. **43**, 2359 (1995).
[5] M. G. Zelin and A. K. Mukherjee, Mater. Sci. Eng., A **208**, 219 (1996).
[6] T. G. Nieh, J. Wadswoth, and O. D. Sherby, *Superplasticity in Metals and Ceramics* (Cambridge University Press, Cambridge, MA, 1997).
[7] S. X. McFadden, R. S. Mishra, R. Z. Valiev, A. P. Zhuyaev, and A. K. Mukherjee, Nature (London) **398**, 684 (1999).
[8] S. X. McFadden, A. P. Zhilyaev, R. S. Mishra, and A. K. Mukherjee, Mater. Lett. **45**, 345 (2000).
[9] H. Van Swygenhoven and A. Caro, Appl. Phys. Lett. **71**, 1652 (1997).
[10] H. Van Swygenhoven and A. Caro, Phys. Rev. B **58**, 11 246 (1998).
[11] H. Van Swygenhoven, M. Spaczer, and A. Caro, Acta Mater. **47**, 3117 (1999).
[12] H. Van Swygenhoven, M. Spaczer, D. Farkas, and A. Caro, Phys. Rev. B **60**, 22 (1999).
[13] H. Van Swygenhoven, D. Farkas, and A. Caro, Phys. Rev. B **62**, 831 (2000).
[14] P. Keblinski, D. Wolf, S. R. Phillpot, and H. Gleiter, Scr. Mater. **41**, 631 (1999).
[15] J. Schiøtz, F. D. Di Tolla, and K. W. Jacobsen, Nature (London) **391**, 561 (1998).
[16] J. Schiøtz, T. Vegge, F. D. Di Tolla, and K. W. Jacobsen, Phys. Rev. B **60**, 11 971 (1999).
[17] *Gmelins Handbuch der Anorganishen Chemie*, edited by A. Kotowski (Springer-Verlag, Berlin, 1967), Vol. 57.
[18] W. Wycisk and M. Feller-Kniepmeier, J. Nucl. Mater. **69**, 616 (1978); **70**, 616 (1978).
[19] H. Conrad and J. Narayan, Scr. Mater. **42**, 1025 (2000).
[20] A. P. Sutton and R. W. Balluffi, *Interfaces in Crystalline Materials* (Oxford Science, New York, 1996).
[21] R. Z. Valiev, V. Yu. Gertsman, and O. A. Kaibyshev, Phys. Status Solidi A **97**, 11 (1986).
[22] D. X. Li, D. H. Ping, J. Y. Huang, Y. D. Yu, and H. Q. Ye, Micron **31**, 581 (2000).
[23] H. E. Schaefer, K. Reimann, W. Straub, F. Phillipp, H. Tanimoto, U. Brossmann, and R. Wurschum, Mater. Sci. Eng., A **286**, 24 (2000).
[24] G. Z. Voronoi, J. Reine Agnew. Math. **134**, 199 (1908).
[25] M. Parrinello and A. Rahman, J. Appl. Phys. **52**, 7182 (1981).
[26] F. Cleri and V. Rosato, Phys. Rev. B **48**, 22 (1993).
[27] M. I. Baskes, X. Sha, J. E. Angelo, and N. R. Moody, Modell. Simul. Mater. Sci. Eng. **5**, 651 (1997).
[28] Y. Mishin, D. Farkas, M. J. Mehl, and D. A. Papaconstantopoulos, Phys. Rev. B **59**, 3393 (1999).
[29] D. J. Honneycutt and H. C. Andersen, J. Phys. Chem. **91**, 4950 (1987).